

MEASUREMENTS OF A SEPARATED AND REATTACHED TURBULENT BOUNDARY LAYER

Jim KOSTAS¹, Julio SORIA¹ and M.S. CHONG²

¹Department of Mechanical Engineering

Monash University, Clayton, Victoria, AUSTRALIA, 3168

²Department of Mechanical and Manufacturing Engineering

Melbourne University, Parkville, Victoria, AUSTRALIA, 3052

ABSTRACT Digital Particle Image Velocity (DPIV) has been used to obtain velocity and vorticity information of a closed separation bubble in a turbulent boundary layer on a flat plate. Separation and reattachment were instigated by imposing an adverse and favourable pressure gradient, respectively, on a turbulent boundary layer. Preliminary observations and measurements indicate a highly unsteady flow with large changes to the shape and size of the separation bubble.

INTRODUCTION

An adverse pressure gradient (APG) can arise from local surface geometry and/or be imposed on a boundary layer by the outer flow. The nature of this APG will determine whether the boundary layer separates, separates and reattaches or does not separate at all.

Flow separation usually occurs at sharp edges of bluff bodies because of the large pressure gradients that exist around these points. At some distance downstream of detachment the separated shear layer may reattach, if the bluff body is sufficiently long. In contrast, a boundary layer on a smooth, flat plate may undergo separation and reattachment if the streamwise pressure gradient is sufficiently adverse and then favourable. This flow situation is more difficult to understand and predict than for bluff body flow since both the separation and reattachment points are not fixed. Previous experimental investigations on a nominally 2-D separating turbulent boundary layer include those by Perry & Fairlie(1975), Simpson *et al.* (1981), Patrick(1987) and most recently Watmuff(1998). Single point interrogation techniques such as hot wire probes and LDA yielded instantaneous pointwise measurements, mean 2-D velocity field measurements and phased averaged 2-D & 3-D velocity measurements in and around the bubble in those studies.

The experimental results described in this paper are concerned with a separating turbulent boundary layer for which the flow was accelerated and then decelerated until separation. The flow is then once again

accelerated so as to achieve reattachment and obtain a closed separation bubble. Instantaneous velocity field and vorticity field measurements in a streamwise plane are presented.

EXPERIMENTAL APPARATUS AND TECHNIQUE Water Tunnel

The experiments were conducted in a closed circuit, horizontal water tunnel, see Fig 1. The test section consists of five 1 m long sections each with a cross-section of 500mm × 500mm. To ensure low turbulence intensities and uniform flow in the test section the settling chamber is equipped with a perforated stainless steel plate followed by four metal screens of decreasing mesh size in the flow direction. A honeycomb section is inserted between the first and second screens to straighten the flow and remove any mean swirl. Finally, a 10:1 contraction is used to further reduce the turbulence intensity by accelerating the mean flow. A maximum flow speed of approximately 1 m/s is achievable in the test section with the 53 kW AC motor and in-line centrifugal pump system. Control of the motor-pump system is done via an ABB Sami GS frequency controller. At the end of the test section a plenum chamber diffuses the flow and returns it via a 300mm diameter pipe to the pump. Perforated stainless steel plates in this plenum chamber, placed vertically and parallel with the test section walls, ensure minimal disturbance to the test section flow as the flow is slowed and redirected through 180 degrees into the return pipe. A diatomaceous earth pool filter system running in parallel with the main return flow pipework removes contaminants from the water. The filtration can be activated at any time but it is never operated during experiments.

A special roof was required in the water tunnel to create the necessary conditions for separation and reattachment of the flow. Figure 1 shows the geometry of the special tunnel roof. The shape is such that the flow is firstly accelerated to a uniform speed and then decelerated so that the boundary layer experiences an APG of sufficient strength to achieve separation. The final region of the roof shape serves

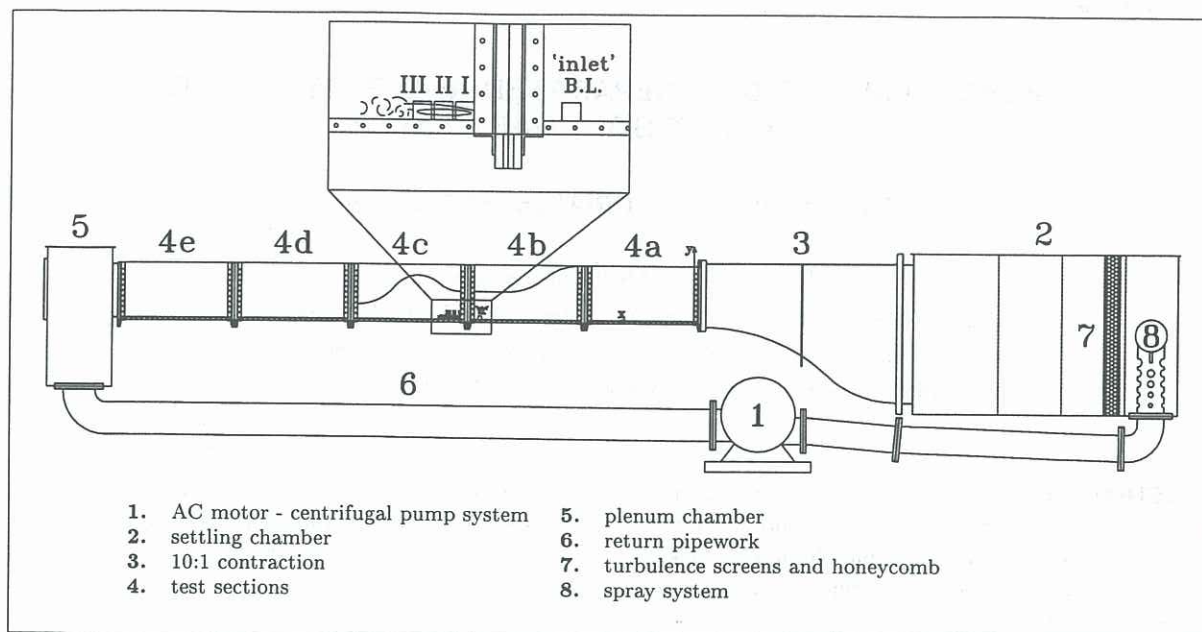


Figure 1: Illustration of the horizontal, closed circuit water tunnel used in the experiments. The arrangement of the screens and honeycomb in the settling chamber is shown. The special roof required for the experiments can be seen in sections 4b and 4c. The measurement regions of the bubble and 'inlet' boundary layer (B.L.) are indicated in the magnified view of the flow region.

to impose a favourable pressure gradient (FPG) on the flow so that it reattaches. Suction was employed on the roof via spanwise slots preventing separation of the boundary layer there. This fluid, removed by suction, was returned to the main settling chamber so that the fluid level does not decrease with time. This arrangement yields a separation bubble approximately 200mm in mean length and 20mm in height.

A mean freestream velocity of $U_\infty = 80 \text{ mm/s}$ (2000mm downstream of the contraction exit) yields Reynolds numbers based on boundary layer thickness, displacement thickness and momentum thickness of $Re_\delta = 1064$, $Re_{\delta^*} = 367$ and $Re_\theta = 152$ respectively. These 'inlet' boundary layer and freestream characteristics were evaluated $\sim 200\text{mm}$ upstream of the separation region, where the flow had been accelerated by the first roof section and had reached a uniform velocity. In this region the boundary layer thickness, displacement thickness and momentum thickness were 11.9mm, 4.1mm and 1.7mm respectively. All results are appropriately non-dimensionalised by the inlet boundary layer displacement thickness and inlet freestream velocity.

PIV Technique

Cross-correlation DPIV of single exposed digital images was used to acquire instantaneous, in-plane velocity field measurements of this flow. A Kodak Megaplex XHF camera coupled to a PC with image acquisition and timing software was used to acquire single exposed images 34 ms apart with a minimum

of 90.2 ms between image pairs. Illumination of the flow was achieved with twin, frequency doubled Nd:YAG lasers each capable of producing a 6ns, 400mJ pulse with a pulse repetition frequency of 12Hz. Firing of the lasers was synchronised with the CCD camera via the control PC. An appropriate combination of cylindrical lenses yielded a 150mm wide by 3mm thick collimated light sheet on entry to the test section. The flow was seeded with $11\mu\text{m}$ hollow glass spheres with a specific gravity of 1.1. Due to the large dimensions of the separation bubble only parts of it could be imaged at a time. A 105mm Micro Nikkor lens placed 500mm from the light sheet provided a field of view of approximately 35mm. The area immediately around the separation region could not be imaged due to interference of the test section flanges. It is estimated that this area is approximately 30mm - 50mm further upstream of the most upstream measurements presented in this paper.

EXPERIMENTAL RESULTS AND DISCUSSION

Observation of the flow revealed the following cycle of events that appeared to repeat every 30 - 60s. A period of stable bubble size and uniform reversed flow was followed by a relatively quick, large growth of the separation bubble by as much as 300%. This was followed by the passage of large scale structures along the shear layer which eventually impinged onto the tunnel floor, causing a violent flapping of the separation bubble. The recirculation region then diminished in size, followed by a growth of the bubble to its nom-

inal size.

Digital particle image velocimetry was used to obtain velocity field measurements just downstream of the separation region. Vorticity field information was extracted from the velocity data using a 13 point χ^2 vorticity calculation method (Fouras & Soria(1998)) with an under-estimation of the peak vorticity due to a bias error of 4.7% and an uncertainty of 1% at a 95% confidence level due to random error. Such measurements for regions I and II are shown in figures 2a and 2b.

An adaptive cross-correlation algorithm developed by Soria(1996) was required to extract the velocity field because of the large dynamic range present in the flow, which was in excess of 100. The spatial resolution of each independent velocity measurement is $0.24\delta^*$ with an uncertainty of $\sigma_u/U_\infty = 0.6\%$.

The vorticity contour plots show isolated concentrations of vorticity present in the shear layer. The somewhat regular spacing is representative of a Kelvin Helmholtz type instability in the shear layer. This has also been observed by Watmuff(1998) for phased averaged measurements with a hot wire in a separated turbulent boundary layer with an inlet Reynolds number of $Re_{\delta^*} = 774$.

Figures 3(a) and 3(b) show instantaneous velocity and vorticity field measurements of the separation bubble in region III during a period in the flow cycle when the separation bubble is experiencing a growth in size. Note the increased reversed flow region in comparison to Figure 2(a). Flow visualisation observations indicate the flow is highly three dimensional. The three dimensionality is most likely due to a spanwise variation in the suction through the roof bleed slots. Further development of the suction system is expected to alleviate this problem.

CONCLUSIONS

From these preliminary PIV measurements it appears that a Kelvin Helmholtz type instability, similar to that for a free shear layer in parallel flow, is present in the shear layer. It is also likely that this instability may eventually lead to the large scale fluctuations observed in the bubble further downstream.

ACKNOWLEDGEMENTS

The financial support of the ARC for this research is greatly appreciated.

REFERENCES

FOURAS, A. & SORIA, J. (1998). Accuracy of out-of-plane vorticity measurements using in-plane velocity vector field data. *Exp. Fluids*. accepted for publication.

PATRICK, W. (1987). Flow field measurements in a separated and reattached flat plate turbulent boundary layer. Technical report NASA. Contractor Report 4052.

PERRY, A. & FAIRLIE, B. (1975). A study of turbulent boundary layer separation and reattachment. *J. Fluid Mech.* **69**, 657-672.

SIMPSON, R., CHEW, Y., & SHIVAPRASAD, B. (1981). The structure of a separating turbulent boundary layer. Part 1. Mean flow and Reynolds stresses. *J. Fluid Mech.* **113**, 23-51.

SORIA, J. (1996). An adaptive cross-correlation digital PIV technique for unsteady flow investigations. In *1st Australian Conference on Laser Diagnostics in Fluid Mechanics and Combustion* (eds. A.R. Masri and D.R. Honnery) University of Sydney, NSW, Australia.

WATMUFF, J. (1998). Evolution of a wave packet into vortex loops in a laminar separation bubble. Technical Report NAS2-14109 Task Number 5 MCAT Inc. NASA Ames Research Center.

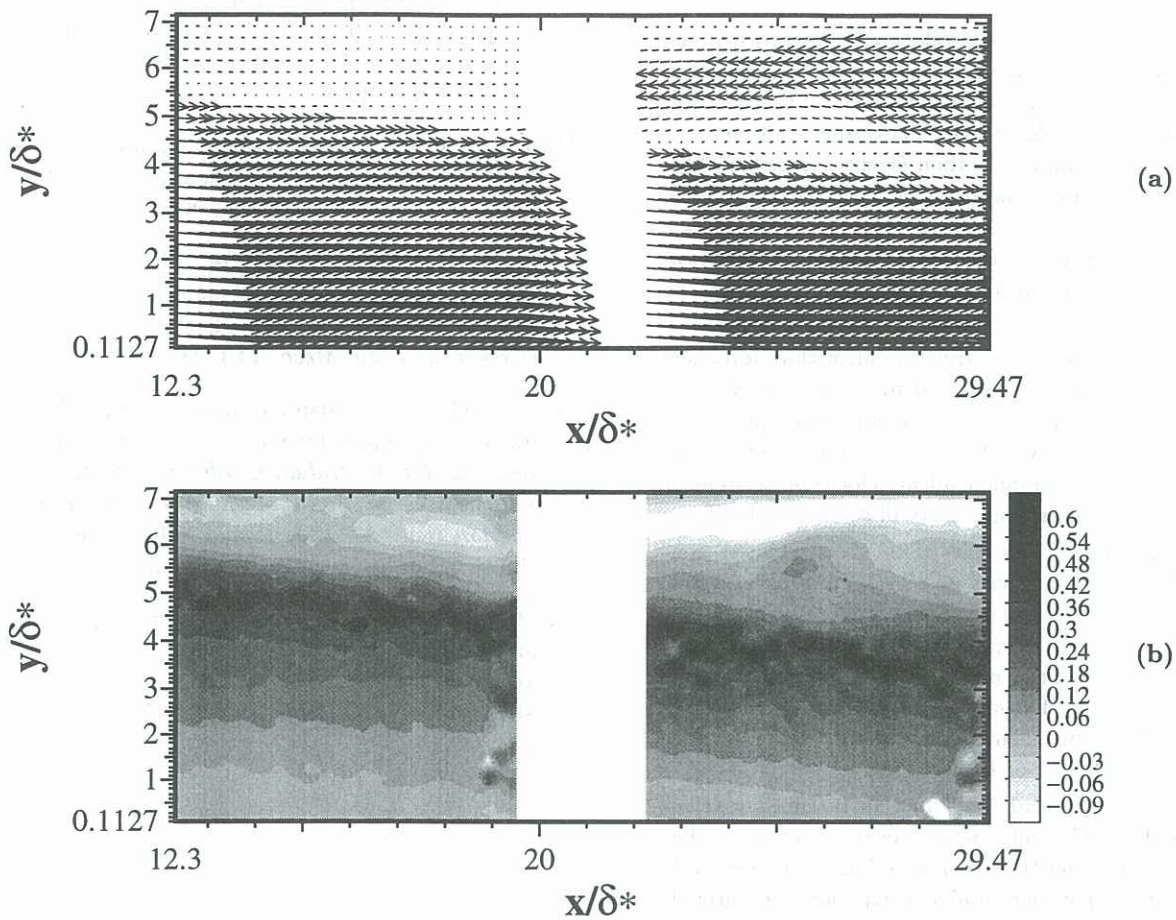


Figure 2: Instantaneous velocity field, (a), and vorticity field, (b), for regions I and II. Flow is from left-to-right. The tunnel floor surface is at the top of each figure. The x-axis represents the downstream distance from the separation region. Freestream velocity, $U_\infty = 80 \text{ mm/s}$, all values nondimensionalised by the inlet boundary layer displacement thickness, δ^* .

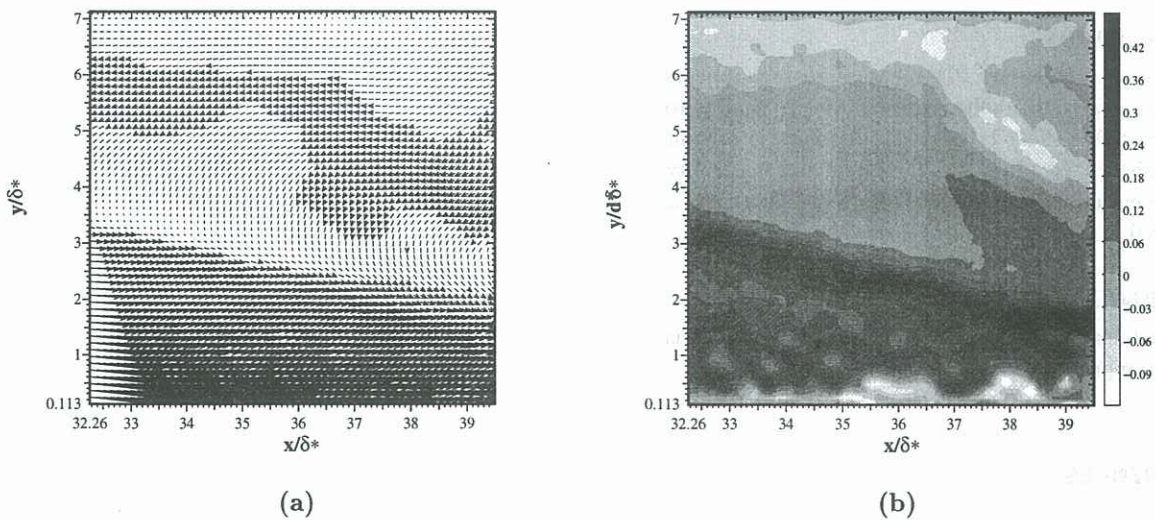


Figure 3: Instantaneous velocity field, (a), and vorticity field, (b), for region III. Flow is from left-to-right. The tunnel floor surface is at the top of each figure. The distance downstream from the separation region is shown on the x-axis. All values nondimensionalised as before.